ACS Photonics

Article

pubs.acs.org/journal/apchd5

# Coupled Mode Modeling To Interpret Hybrid Modes and Fano Resonances in Plasmonic Systems

Saïd Bakhti, Nathalie Destouches,* and Alexandre V. Tishchenko

University of Lyon, F-42023 Saint-Etienne, France

Laboratoire Hubert Curien, CNRS, UMR 5516, 18 Rue Pr. Lauras, F-42000 Saint-Etienne, France

University of Saint-Etienne, Jean Monnet, F-42000 Saint-Etienne, France

Supporting Information

**ABSTRACT:** By generalizing the concept of extinction cross-section to complex valued extinction cross-section we analyze the coupling between plasmon modes in metallic dimers or quadrumers. Identifying the phase information in the field scattered by subsets of the whole plasmonic system allows to infer the formation of subradiant or super-radiant hybrid modes. We also propose a phenomenological modeling based on the use of coupled mode equations to deduce from rigorous calculations a quantitative estimate of mutual coupling coefficients when only two modes interfere. These coefficients determine the spectral position of hybrid modes. This approach is applied to two interacting silver spheres; the parameters of the energetic diagram are calculated as a function of the gap between spheres. In the case of two identical spheres illuminated with a linearly polarized light parallel or perpendicular to the dimer, only one hybrid mode is excited. The phenomenological modeling is then applied to a four-particle system, where the interaction between the initial dipolar modes gives rise to Fano resonances. In a weak coupling regime of the system, the asymmetric line profile in the extinction spectra of the system emerges from the superposition of a broad super-radiant mode and a sharp subradiant mode. A strong coupling regime is characterized by a broadened subradiant mode and a larger Fano resonance. The sharpness of the Fano resonance in the weak coupling regime makes this structure well suited for sensing applications.

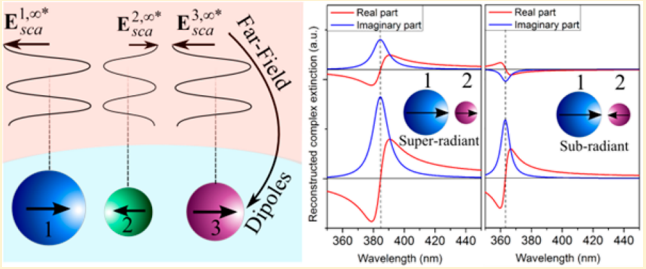


**KEYWORDS:** *coupled mode model, plasmon resonances, metal nanoparticles, hybrid modes, Fano resonances*

Metal nanoparticles (NPs) have been attracting an increasing attention for few decades, particularly due to their unique optical properties. Localized surface plasmon resonances (LSPRs) occurring on such NPs under an electromagnetic excitation result from a coupling between the incident wave and the surface charge density oscillations of particles.[1] The resonant behavior of a single metal particle depends on many physical and geometrical parameters. The nature of the metal affects the spectral range of resonances. Noble metal particles and, particularly, silver and gold are well-known to resonate in the visible range, making such materials particularly well suited for practical applications.[2] The particle size and shape, as well as the optical properties of the surrounding medium, also influence the spectral response of nanoparticles. The number of excited resonant modes, their nature, and their spectral location mainly depend on the particle geometry,[3,4] whereas the host medium refractive index shifts the resonance wavelength.[5,6] Each resonant mode corresponds to a discrete coupling state between the incident radiation and a surface charge oscillation mode and appears in the particle spectral response as a resonance band with a center wavelength and a finite full width at half-maximum (fwhm). Excitation of a given mode leads to an enhancement in the radiative (scattering) and nonradiative (absorption) response of the particle, providing large intensities in the close proximity of particles[7] with a mode dependent spatial distribution. The spectral behavior of LSPRs together with their sensitivity to the ambient medium and the possibility to confine light at the nanoscale make metal NPs powerful in a broad range of applications, including biological and chemical sensing,[8] surface-enhanced Raman spectroscopy,[9] nanophotonics,[10] or improved photovoltaic devices.[11]

Among all properties of LSPRs, the coupling between two or more particles offers a promising way to design specific optical responses. In the simple case of two close particles in strong interaction, the dimer response results from a coupling between the different modes of individual particles and is characterized by spectral shifts from individual resonances and generally by a larger field enhancement between the particles. The dimer resonance modes then differ from the individual particle ones according to the nature of the coupling and its strength. A physical description of interactions in plasmonic resonant systems is provided by the hybridization theory.[12] In the general case, this approach considers the modes of a system of

**Received:** September 28, 2014
**Published:** January 6, 2015





DOI: 10.1021/ph500356n
*ACS Photonics* 2015, 2, 246−255

particles as hybrid modes resulting from bounding and antibounding combinations of the individual particle modes,[13] as we generally deduce the molecular orbitals from the atomic orbitals.[14] Under certain configurations, plasmonic particle systems can have Fano-like resonances in their optical response,[15,16] that is, resonances with an asymmetric line shape that differs from the Lorentzian profile generally used to describe the LSPRs. Fano resonances result from interactions between a discrete state and a continuum of states, where destructive and constructive interferences occur depending on the wavelength.[17] In metal NP assemblies, Fano-like resonances are due to interferences between strongly coupled narrow and broad resonances and appear in structures like particle oligomers,[18] disk/ring assemblies,[19] or dolmen-like structures.[20]

In this paper, we propose to extend the concept of extinction cross-section to complex valued extinction to analyze the coupling between plasmon modes in metallic dimers and quadrumers. This complex quantity gives access to the phase information resulting from the interaction of the scattered field with the incident one and can be calculated for a subset of each considered plasmonic system. The contribution of each particle of a dimer to a plasmon mode is therefore rigorously calculated in a complex form and the nature of interferences resulting from the interaction between all contributions is predicted according to the sign of their real part. A phenomenological approach is also developed on the basis of coupled-mode equations to deduce mutual coupling coefficients from the resonance parameters rigorously calculated. This approach is applied to two interacting silver spheres to identify and characterize the coupling-induced hybrid modes. A more complex system consisting in a quadrumer exhibiting Fano-like resonances is further studied. In this case, the coupling occurring between the four particles is also well interpreted with the phenomenological approach.

## CALCULATION OF THE COMPLEX VALUED EXTINCTION

A practical way to characterize the optical response of a particle system is to introduce the optical cross sections.[21] In particular, the extinction cross-section $C_{ext}$ expresses the total power losses in the system due to absorption and scattering processes. In the case of a single particle, this quantity is expressed using the so-called optical theorem

$$C_{ext} = \frac{4\pi}{k_s |\mathbf{E}_0|^2} \mathrm{Im}[\mathbf{E}_0^* \cdot \mathbf{E}_{sca}^{\infty}(\mathbf{e}_k)] \quad (1)$$

where $\mathbf{E}_{sca}^{\infty}(\mathbf{e}_k)$ is the far-field scattered in the forward direction $\mathbf{e}_k$ of the incident field. The latter is assumed here to be a monochromatic incident plane wave $\mathbf{E}_{inc} = \mathbf{E}_0 \exp(j\mathbf{k}_s \cdot r)$ of pulsation $\omega$ traveling in the surrounding medium of refractive index $n_s$ with wave vector $k_s$. For a many-particle system, the total extinction cross-section can be defined as the sum of the individual particle extinction cross sections.

Here, we propose to generalize the concept of extinction cross-section, by introducing the complex valued extinction $\tilde{C}_{ext}^i$ for each particle and $\tilde{C}_{ext}$ for the system on the basis of the classical extinction cross-section defined in eq 1

$$\tilde{C}_{ext} = \sum_i \tilde{C}_{ext}^i = -\sum_i \frac{4\pi}{k_s |\mathbf{E}_0|^2} \mathbf{E}_0 \cdot \mathbf{E}_{sca}^{i,\infty *}(\mathbf{e}_k) \quad (2)$$

where $\mathbf{E}_{sca}^{i,\infty}(\mathbf{e}_k)$ is the far-field scattered by the $i$th particle of the system. The optical theorem expressed in eq 1 defines the extinction cross-section as an attenuation of the incident radiation due to its interference with the scattered field in the forward direction. In contrast to the classical quantity, the complex valued extinction defined in eq 2 also gives access to the phase information resulting from the interaction of the scattered field with the incident one. Even if the individual contributions $\tilde{C}_{ext}^i$ to the total extinction do not represent any measurable quantity, they allow characterizing the contribution of each particle to the optical response of the global system. In order to interpret the resonance curves, we show the phase as well as the real and imaginary parts of the individual complex valued extinctions, noting that the imaginary part corresponds to the classical extinction cross-section. The phase of the complex valued extinction is the same as the dipolar moment oscillation. We remind that, in the case of a dipolar resonance, the phase of the dipolar moment matches the phase of the incident field at energies lower than the resonance and is out-of-phase at higher energies.

The partial complex extinctions provide information about the relative oscillations of resultant dipolar moments of the particles. When particles are illuminated with a constant phase of the incident plane wave (Figure 1), the phase difference

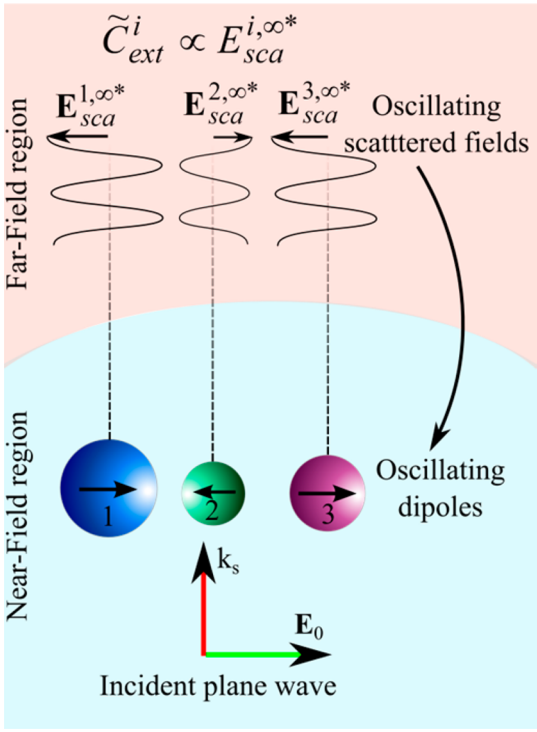


**Figure 1.** Schematic representation of phase relations between partial scattered fields and oscillating dipolar moments of a system of particles.

between their scattered far-field (and, hence, between their partial complex extinction, according to eq 2) results from a phase difference in their dipolar moments. Complex extinction can then be conveniently used to characterize the radiative behavior of each particle of a coupled system.

## PHENOMENOLOGICAL DESCRIPTION OF PLASMON RESONANCES

We derive in this section a set of phenomenological equations driving the amplitude of coupled plasmon modes, with a few


DOI: 10.1021/ph500356n
ACS Photonics 2015, 2, 246−255

parameters characterizing the coupling behavior in simple plasmonic systems. The proposed formalism is consistent with the classical coupled mode theory.[22]

As demonstrated in our previous work,[23] a single plasmon mode can be described through a first order differential equation driving the mode amplitude $a(t)$ excited by an incident radiation (like an incident electric field) $f_0(t)$

$$\frac{da(t)}{dt} = -j\mathrm{Re}\{\omega_p\}a(t) - \frac{1}{\tau}a(t) + \kappa f_0(t) \tag{3}$$

where $\tau$ is the time decay of the plasmon (representing the total losses in the system), $\kappa$ is the coupling coefficient, and $\omega_p$ is the complex resonant pulsation of the plasmon mode. The real part of $\omega_p$ corresponds to the resonance position and the imaginary part to its half width at half-maximum. Considering both the incident radiation and the plasmon amplitude oscillating with the pulsation $\omega$, such quantities can be expressed in terms of their modulation amplitudes $\tilde{f}_0(t)$ and $\tilde{a}(t)$, respectively

$$\begin{cases} f_0(t) = \tilde{f}_0(t)\ \exp\{-j\omega t\} \\ a(t) = \tilde{a}(t)\ \exp\{-j\omega t\} \end{cases} \tag{4}$$

By including these expressions in eq 3 and by fixing the condition $\tilde{f}_0(t) = 1$, which corresponds to the case of a plane wave excitation with unit amplitude, we obtain the following particular solution of eq 3 in the steady state

$$\tilde{a}(\omega) = \frac{j\kappa}{\omega - \mathrm{Re}\{\omega_p\} + \left(j/\tau\right)} \tag{5}$$

The modulation amplitude $\tilde{a}$ then only depends on the pulsation $\omega$, and the obtained expression can be written as a simple singular function

$$\tilde{a}(\omega) = \frac{a_p}{\omega - \omega_p} \tag{6}$$

where the coupling coefficient is related to the amplitude by $a_p = j\kappa$, and the time decay to the imaginary part of the complex pulsation by $\mathrm{Im}\{\omega_p\} = -1/\tau$. Regarding eqs 3 and 5, the complex valued coupling coefficient quantifies the coupling between the incident excitation and the plasmon mode. Its amplitude provides the coupling strength, and its phase corresponds to the oscillator phase at resonance relative to the excitation.

This formulation can be applied to plasmon modes in single or noninteracting particles. In the case of close particles, plasmon resonances strongly interact, resulting in the formation of hybrid modes in the particle system. In order to generalize the phenomenological description to coupled systems, we consider the simplest case of two interacting plasmon modes. In such a case, we can write the coupled mode equations on the basis of the single mode equation. Considering two coupled modes $a_1(t)$ and $a_2(t)$ with original complex pulsations $\omega_1$ and $\omega_2$, coupled to the incident radiation with coupling coefficients $\kappa_1$ and $\kappa_2$, the phenomenological equations driving these modes can be given by

$$\begin{cases} \dfrac{da_1(t)}{dt} = -j\mathrm{Re}(\omega_1)a_1(t) + \mathrm{Im}(\omega_1)a_1(t) + \kappa_1 f_0(t) \\ \qquad\qquad + \kappa_{12}a_2(t) \\ \dfrac{da_2(t)}{dt} = -j\mathrm{Re}(\omega_2)a_2(t) + \mathrm{Im}(\omega_2)a_2(t) + \kappa_2 f_0(t) \\ \qquad\qquad + \kappa_{21}a_1(t) \end{cases} \tag{7}$$

with $\kappa_{12}$ and $\kappa_{21}$ the mutual coupling coefficients between the two modes. As in the case of a single mode, the plasmon amplitudes can be expressed in the following form:

$$\begin{cases} a_1(t) = \tilde{a}_1(t)\ \exp\{-j\omega t\} \\ a_2(t) = \tilde{a}_2(t)\ \exp\{-j\omega t\} \end{cases} \tag{8}$$

Injecting relation 8 into 7, the particular solutions of the coupled mode equations in steady state, and when $\tilde{f}_0(t) = 1$, can be written as

$$\begin{cases} \tilde{a}_1(\omega) = \left[\dfrac{a_1^+}{\omega - \omega^+} + \dfrac{a_1^-}{\omega - \omega^-}\right] \\ \tilde{a}_2(\omega) = \left[\dfrac{a_2^+}{\omega - \omega^+} + \dfrac{a_2^-}{\omega - \omega^-}\right] \end{cases} \tag{9}$$

These solutions appear as a sum of two singular functions, showing that the coupling between the plasmon modes results in two hybrid modes with complex resonance pulsations $\omega^+$ and $\omega^-$ distinct from the original mode pulsations. The values of the resonance parameters $a_1^-$, $a_1^+$, $a_2^-$, $a_2^+$, $\omega^+$, and $\omega^-$ of these hybrid modes can be calculated after fitting the optical response of the system with a meromorphic function of the pulsation with two singular points.[24] All phenomenological parameters introduced in eqs 7 can then be expressed as a function of the resonance parameters of hybrid modes. The coupling coefficients are given by

$$\begin{cases} \kappa_1 = -j(a_1^+ + a_1^-) \\ \kappa_2 = -j(a_2^+ + a_2^-) \end{cases} \tag{10}$$

Since these coefficients have to be constant for the given modes $a_1(t)$ and $a_2(t)$, the sum of hybrid mode amplitudes $a_1^+ + a_1^-$ and $a_2^+ + a_2^-$ remains constant, whatever the coupling state between the plasmon modes. The mutual coupling coefficients are given in turn by

$$\begin{cases} \kappa_{21} = -\dfrac{a_2^+ a_2^-}{a_1^+ a_2^- - a_1^- a_2^+}\Delta\omega^\pm \\ \kappa_{12} = \dfrac{a_1^+ a_1^-}{a_1^+ a_2^- - a_1^- a_2^+}\Delta\omega^\pm \end{cases} \tag{11}$$

with $\Delta\omega^\pm = \omega^+ - \omega^-$. Considering that these coupling coefficients reflect the coupling strength in the system and regarding their expressions, the difference between the complex pulsation of hybrid modes, $\Delta\omega^\pm$, as well as the product of their amplitude, give a direct measure of the coupling effects in particle aggregates. As for the coupling coefficients, the mutual coupling coefficients are complex valued parameters whose amplitude provides a direct estimate of the coupling strength between the particles, and phase corresponds to the phase detuning with which a mode acts on the other.

Finally, the original and hybrid mode pulsations are related as


DOI: 10.1021/ph500356n
ACS Photonics 2015, 2, 246−255

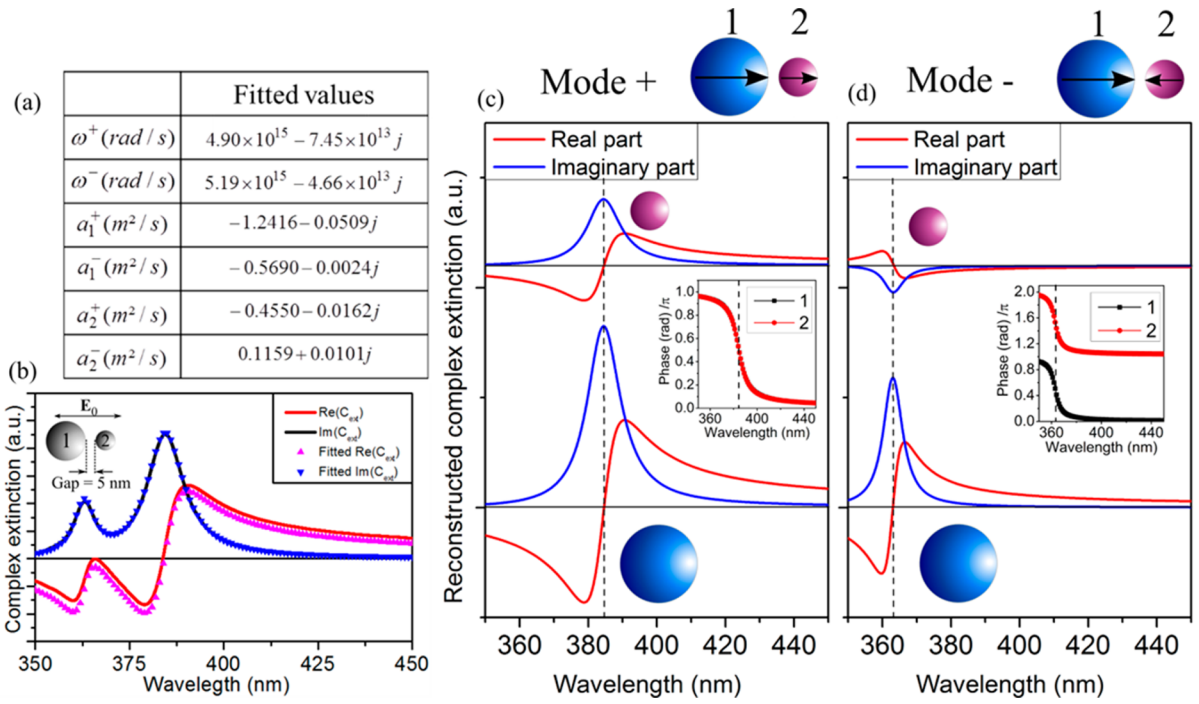


**Figure 2.** (a) Resonance characteristics of hybrid modes for a dimer composed of 20 and 10 nm in radius spheres, with a gap of 5 nm. (b) Comparison of the total complex extinction cross sections calculated from a rigorous approach and from singular functions of c and d. (c, d) Contribution of each particle to the extinction of each hybrid mode (these two graphs have the same ordinate amplitude).

$$\begin{cases} \omega^+ = \omega_1 + j\dfrac{a_2^+}{a_1^+}\kappa_{12} \\ \omega^- = \omega_2 + j\dfrac{a_1^-}{a_2^-}\kappa_{21} \end{cases} \tag{12}$$

These relations show that, for given original modes, the shift of hybrid modes directly depends on the mutual coupling coefficients, as expected in strongly coupled oscillators.[25]

Consider now the limit of uncoupled modes, for example, by sufficiently distancing two particles so that they no longer interact with each other. The mutual coupling coefficients should nullify and the equations in 7 become independent. In this case, the nullification of the two hybrid mode amplitudes $a_1^-$ and $a_2^+$ ensure that the mutual coupling coefficients nullify and that the hybrid mode pulsations tend to the original ones ($\omega^+ \to \omega_1$ and $\omega^- \to \omega_2$).

The formalism presented here concerns the coupling between two modes only, whereas realistic cases often present more complex coupling behavior. However, this simple model helps to predict and to analyze hybrid modes in dimers as well as Fano resonances appearing in strongly coupled systems, as shown hereafter. It will be applied to fit the complex extinction spectra in silver nanoparticle based structures. The details related to the method used to compute the rigorous extinction as well as the silver permittivity model can be found in Methods.

## HYBRID MODES IN DIMERS

We start the analysis of plasmon modes in dimers by first considering two spheres of 20 nm (S1) and 10 nm (S2) in radius, with a gap of 5 nm between their surfaces and illuminated by a plane wave polarized parallel to the dimer axis. These particles are small enough to mainly exhibit a dipolar resonance when taken separately. We compute separately, from the rigorous resolution of the multiple scattering problem, the partial complex extinctions $\tilde{C}_{ext}^1$ and $\tilde{C}_{ext}^2$ of S1 and S2. Each of these complex quantities exhibits two resonances expected to correspond to hybrid modes resulting from the coupling between the dipolar modes of particles. Fitting their spectral variations with a meromorphic function (being the sum of two singular functions), as described in eq 9, gives the values of the hybrid pulsations $\omega^+$ and $\omega^-$ and amplitude parameters $a_1^-$, $a_1^+$, $a_2^-$, and $a_2^+$ (Figure 2a). The reconstruction of each singular function of eq 9 from the extracted parameters is shown in Figure 2c,d. These curves correspond to the contribution of each particle to each hybrid mode. The sum of all these functions, which corresponds to the total complex valued extinction of the system, is compared to the spectral variations calculated rigorously in Figure 2b. The good agreement between the curves proves that the phenomenological approach is accurate for this system.

Looking at the separated contributions of S1 and S2 to each hybrid mode in Figure 2c,d also inform on the nature of these modes. When the phase of the singular functions corresponding to S1 and S2 are the same, their mode can be interpreted as resulting from dipoles oscillating in phase (Figure 2c). We can note here that the same sign of the real and imaginary part of the singular functions can also be interpreted as in-phase dipolar oscillations. This results in a large dipolar moment and a highly radiative system whose mode is qualified of super-radiant. When the real or the imaginary parts have opposite signs (Figure 2d), the dipolar moments of both particles oscillate out-of-phase leading to a small resulting dipolar moment of the dimer and to a poorly radiative system. The mode is then said to be subradiant. The resonance bandwidth of a given mode is related to the total losses in the system. In the case of a subradiant mode, the reduced resulting dipolar moment results in lower radiative losses, leading to a sharper


DOI: 10.1021/ph500356n
ACS Photonics 2015, 2, 246−255

resonance bandwidth. For a super-radiant mode, the opposite effect is observed, and the highly radiative behavior results in high radiative losses and hence to a broader resonance bandwidth. These behaviors appear in the two hybrid modes of the dimer.

Similar results are obtained when considering an incident polarization perpendicular to the dimer axis, where both subradiant and super-radiant modes are identified from the fitted resonance characteristics (see Figure S1 in Supporting Information).

An interesting effect of hybrid modes relies on the near-field around the particles. Then, in the case of the super-radiant mode, all particles radiate in-phase, leading to constructive interferences on the total field between the particles. As an example, this effect is at the origin of "hot spots" in the gap of a dimer when illuminating it with a parallel polarization. For subradiant modes, the out-of-phase radiation of the particles leads to destructive interferences and then to a minimal intensity of the local field.

An important feature in coupled systems is the dependence of the coupling strength with the distance separating the particles. Following the phenomenological analysis in the previous section, the mutual coupling coefficients can serve to quantify the interaction between nanoparticles. Figure 3 depicts

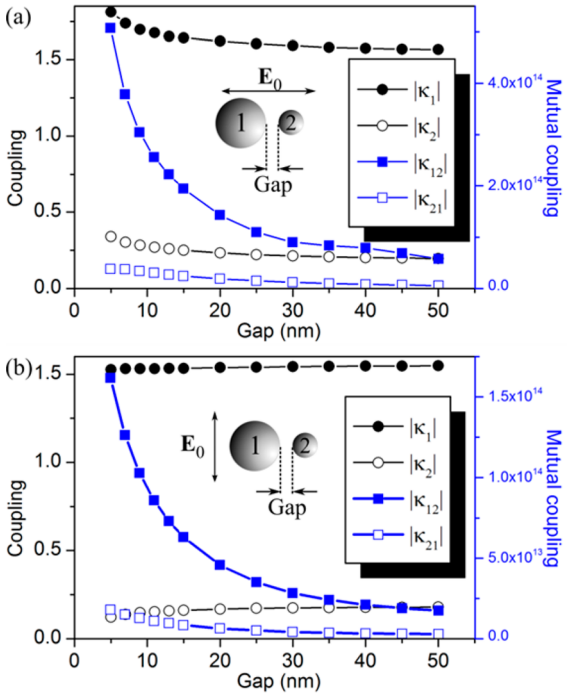


**Figure 3.** Coupling (on the left *y*-axis) and mutual coupling (on the right *y*-axis) coefficients vs the gap between particles for an incident polarization (a) parallel or (b) perpendicular to the dimer axis.

the modulus of both coupling and mutual coupling coefficients as a function of the gap between the particles, for an incident polarization parallel or perpendicular to the dimer axis. Coupling coefficients $\kappa_1$ and $\kappa_2$ are intrinsic characteristics of each sphere and then are expected to be independent of the dimer configuration. However, the plotted values show a slight decrease of these coefficients with increasing the gap. This can be interpreted as a consequence of coupling between dipolar modes and higher order modes. Indeed, the phenomenological analysis of the system only consider the ideal case of coupling between two (here dipolar) modes. Actually, coupling between dipolar and quadrupolar modes also occurs, inducing disparities between expected and computed phenomenological values.

The computed mutual coupling coefficients $\kappa_{12}$ and $\kappa_{21}$ show for each incident polarization a fast decreasing coupling strength when increasing the gap between particles. By comparing the amplitudes for each polarization, the coupling strength in the case of a parallel polarization appears to be larger (by a factor of about 3) than in the perpendicular case. When considering each sphere as oscillating dipoles, this result indicates a better coupling in the case of parallel dipolar moments. Regarding again the coupling coefficients, their values are more perturbed for a parallel incident polarization. In this case and for close particles, relatively strong coupling effects can be expected between dipolar and higher order modes, compared with a perpendicular polarization, where the coupling coefficients are more stable.

We can note here the different orders of magnitude between the coupling and mutual coupling coefficients. This difference comes from the different physical inputs to which they apply: $\kappa_1 f_0(t)$, $\kappa_2 f_0(t)$, $\kappa_{12} a_2(t)$, and $\kappa_{21} a_1(t)$. These terms have the same dimension, and their comparison could inform about the relative importance of the coupling and mutual coupling effects in the resonant behavior of the system.

The hybrid modes resulting from the coupling between particles resonate at complex pulsations $\omega^+$ and $\omega^-$ different from the pulsation of initial modes $\omega_1$ and $\omega_2$. Their determination gives an energetic diagram of the system, as shown in Figure 4a. The latter highlights different behaviors of hybrid modes. The two modes resonating at higher wavelengths (and lower energy) are red-shifted when increasing the interparticle coupling. They correspond to an energetically favorable configuration of the dipolar moments of the particles, that is, when the dipoles are attractive. These modes can be seen as bounding states of the system (Figure 4c). The modes resonating at lower wavelengths correspond to a repulsive configuration of dipoles and can be seen in turn as antibonding states of the system. Another interesting feature is that the resonance position of bonding states tends to the dipolar mode position of the larger particle, whereas the resonance position of antibonding states tends to the dipolar mode position of the smaller particle.

Consider now the special case of homodimers, composed of identical particles. In such a case, the initial modes have identical coupling coefficients $\kappa_0$ with the incident excitation and resonate at the same pulsation $\omega_p$. Anticipating the mutual coupling coefficients to be equal ($\kappa_{12} = \kappa_{21} = \kappa$), as well as the mode amplitudes ($a_1(t) = a_2(t) = a(t)$), the coupled mode eq 7 can be simplified in a single equation:

$$\frac{da(t)}{dt} = -j\mathrm{Re}\{\omega_p\}a(t) + \mathrm{Im}\{\omega_p\}a(t) + \kappa a(t) + \kappa_0 f_0(t) \tag{13}$$

Included in eq 13 is the expression of the mode amplitude given by eq 4, which yields in steady-state the condition $\tilde{f}_0(t) = 1$

$$\tilde{a}(\omega) = \frac{j\kappa_0}{\omega - \omega_p - j\kappa} = \frac{a^+}{\omega - \omega^+} \tag{14}$$

As a consequence, the coupling between two identical particles leads to a single hybrid mode with a complex pulsation


DOI: 10.1021/ph500356n
ACS Photonics 2015, 2, 246−255

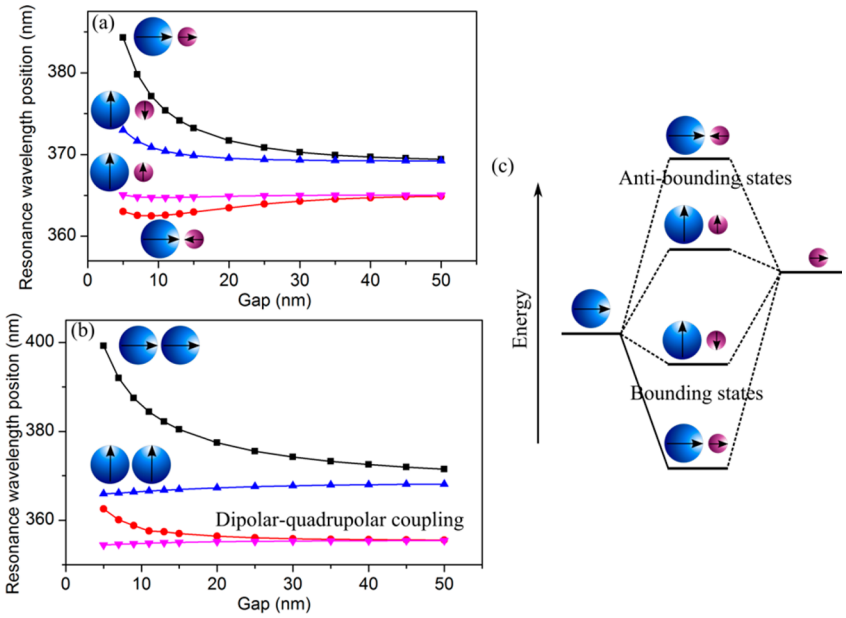


**Figure 4.** Resonance position of hybrid modes versus the gap between particles for a dimer composed of (a) 10 and 20 nm in radius spheres and (b) identical spheres 20 nm in radius. (c) Schematic representation of the energetic repartition of hybrid modes.

$\omega^+ = \omega_p + j\kappa$ and a resonance amplitude $a^+ = j\kappa_0$. This hybrid mode has the same amplitude as the initial mode, and the resonance pulsation is only shifted from the initial position $\omega_p$ by the mutual coupling term $j\kappa$. Obviously, the resonant response of both particles is exactly the same, and the hybrid mode corresponds systematically to a super-radiant mode (in-phase oscillations). Out-of-phase oscillations of dipolar moments appear as forbidden (i.e., dark) modes.

The energetic diagram of a homodimer composed of 20 nm in radius spheres is plotted in Figure 4b. In addition to the identified hybrid modes, different modes resulting from a coupling between dipolar and quadrupolar initial modes are also represented. For a complete description of these interactions with higher modes, the phenomenological description used has to be generalized to the case of $M$ cross-coupled modes.

## FANO RESONANCES IN QUADRUMERS

We deal now with another system where strong coupling between plasmon modes occurs. This system is schematically described in Figure 5, and consists in a quadrumer composed of identical spherical particles 30 nm in radius. This system can be viewed as a pair of vertical (D1) and horizontal (D2) homodimers. When illuminating this system with an incident plane wave polarized along the D2 axis, the original particle modes are strongly coupled. The extinction spectra calculated from the rigorous resolution of the multiple scattering problem are plotted in Figure 5 versus the gap of D2. They exhibit Fano resonances, that is, asymmetric resonant line profiles, in the extinction cross-section spectra, noting also the presence of a quadrupolar resonance at about 360 nm.

In order to analyze the coupling effects in the quadrumer, we consider eqs 7 extended to four coupled equations to describe the mutual coupling between the four particles. Due to the symmetry of this system and considering the given incident polarization, these equations can be reduced into two coupled equations describing the resonance behavior of the quadrumer

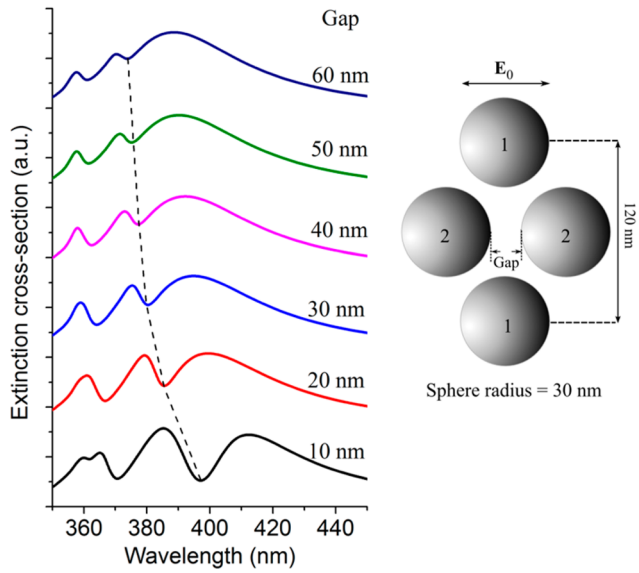


**Figure 5.** Extinction cross-section of the system sketched on the right composed of two interacting dimers, versus the gap of the horizontal dimer. The dashed line indicates the position of the Fano dips in the extinction spectra.

$$\begin{cases} \dfrac{da_1(t)}{dt} = -j\mathrm{Re}(\omega_0)a_1(t) + \mathrm{Im}(\omega_0)a_1(t) + \kappa_0 f_0(t) \\ \qquad + \kappa_{11}a_1(t) + 2\kappa_{12}a_2(t) \\ \dfrac{da_2(t)}{dt} = -j\mathrm{Re}(\omega_0)a_2(t) + \mathrm{Im}(\omega_0)a_2(t) + \kappa_0 f_0(t) \\ \qquad + \kappa_{22}a_2(t) + 2\kappa_{12}a_1(t) \end{cases} \quad (15)$$

where $a_1(t)$ and $a_2(t)$ are the resonance amplitudes in the dimers D1 and D2, respectively. $\omega_0$ is the original complex pulsation of the particles' dipolar resonance and $\kappa_0$ is their coupling coefficient with the incident radiation. $\kappa_{11}$ and $\kappa_{22}$ are the mutual coupling coefficients between the particles in the dimers D1 and D2, respectively, $\kappa_{12}$ is the mutual coupling coefficient between the D1 and D2 particles. The coupled eqs


DOI: 10.1021/ph500356n
ACS Photonics 2015, 2, 246−255

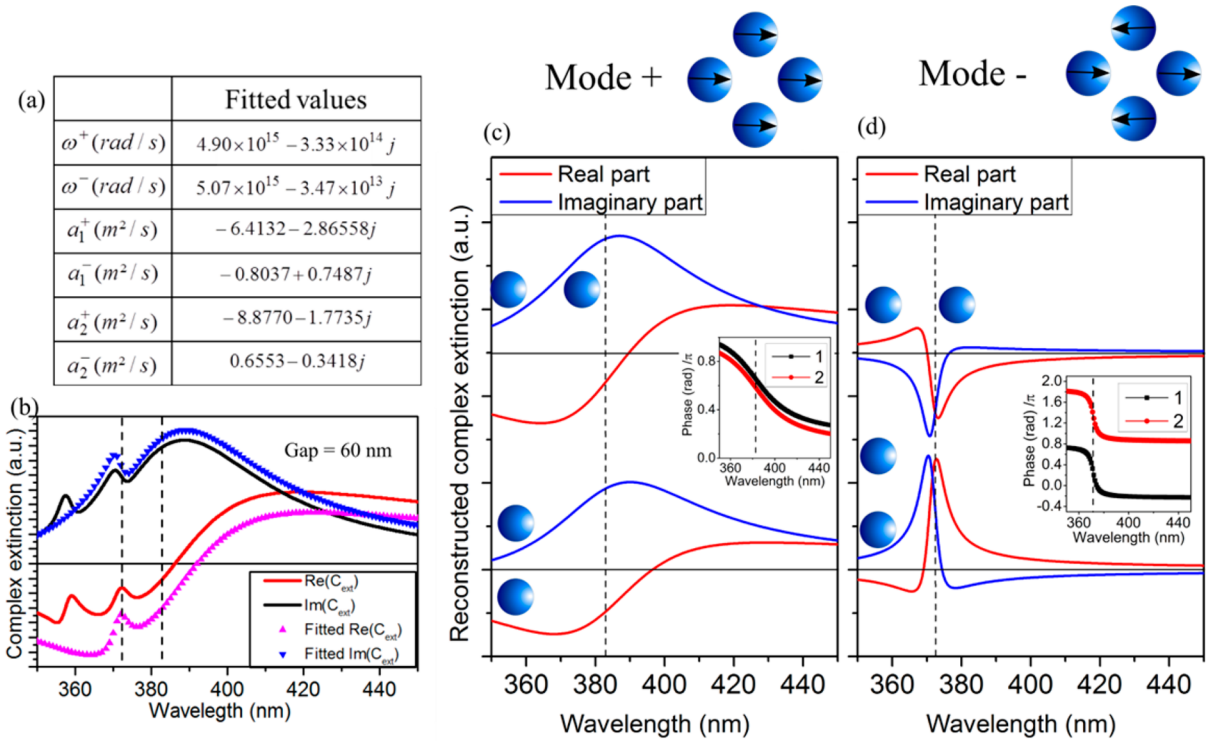


**Figure 6.** (a) Resonance characteristics fitted from the partial complex valued extinction cross-section of each dimer. The gap of D2 is fixed to 60 nm. (b) Total complex extinction cross-section from rigorous calculation and the phenomenological modeling. (c, d) Singular functions giving the contribution of each dimer to each hybrid mode (these two graphs have the same ordinate amplitude).

15 describing the system anticipate the formation of two different hybrid modes from the coupling of the initial dipolar resonances of the particles.

In order to determine the coupling characteristics of such a quadrumer, we compute the partial complex extinction cross sections of each dimer $\tilde{C}_{ext}^{D1}$ and $\tilde{C}_{ext}^{D2}$. The resonance parameters of the hybrid modes (for a gap of 60 nm in D2) are gathered in Figure 6a, and the reconstructed singular functions corresponding to the contribution of each dimer to both hybrid modes are shown in Figure 6c,d. The sum of all these contributions, deduced from the phenomenological approach, is in good agreement with the total complex valued extinction cross-section calculated rigorously (Figure 6b), except for the quadrupolar mode (at about 355 nm) not taken into account in our model. This proves the validity of the coupled-mode approach for this kind of system too.

As previously stated, the nature of hybrid modes can be identified through the phase shifts between the dipolar oscillations deduced from singular functions plotted in Figure 6c,d. For the hybrid mode resonating at angular frequency $\omega^+$, the dipolar modes associated with D1 and D2 oscillate nearly in phase (Figure 6c). This hybrid mode corresponds therefore to a high resultant dipolar moment making this mode highly radiative and qualified of super-radiant. The hybrid mode resonating at $\omega^-$ is characterized by an out-of-phase oscillation of the dipolar moments, making this mode poorly radiative that can be qualified of subradiant. A particular feature of this system comes from highly asymmetric line profiles in the contribution of both dimers to the subradiant mode. The superposition of these asymmetric line profiles with the contribution of the super-radiant mode explains the Fano line-shape in the total extinction of the quadrumer.

Figure 7a shows the plot of relative dipolar moment phases for the two hybrid modes in function of the gap in D2, revealing two different coupling regimes. When increasing the gap between the particles in D2 (corresponding to weak coupling), the super-radiant mode tends to a zero phase shift between all the dipolar moments resulting in a large bandwidth (Figure 7c), and the subradiant mode tends to a $\pi$ phase shift with a reduced bandwidth. This regime results in a sharp Fano resonance in the extinction spectra (Figure 5). In the strong coupling regime, that is, when reducing the gap in D2, a reduction in the phase shifts of the super-radiant mode is observed, while its bandwidth is reduced. Contrarily, the phase difference between the dipolar moments of the subradiant mode tends to be reduced and its bandwidth increases. Then under this regime the super-radiant and subradiant modes become, respectively, less and more radiative. Moreover, the plot of the spectral position of these hybrid modes (Figure 7b) shows that the difference between their spectral positions decreases with the gap in D2. The combination of these two modes forms a broader Fano resonance in the structure total extinction spectrum.

An actual interest of Fano resonances in plasmonic structures lies in their extreme sensitivity to the local environment, making such resonances well suited for sensing applications. The sensing capabilities of plasmon resonances can be evaluated through their Figure of Merit[26] (FoM), defined as the ratio of the plasmon energy shift per refractive index unit change in the surrounding medium, divided by the width of the resonance band. Since the FoM of a given mode mainly depends on its spectral width, the Fano resonance of the quadrumer in the weak coupling regime appears as the best configuration for sensing because of its sharp width compared to the Fano resonance in the strong coupling regime. The plot


DOI: 10.1021/ph500356n
ACS Photonics 2015, 2, 246−255

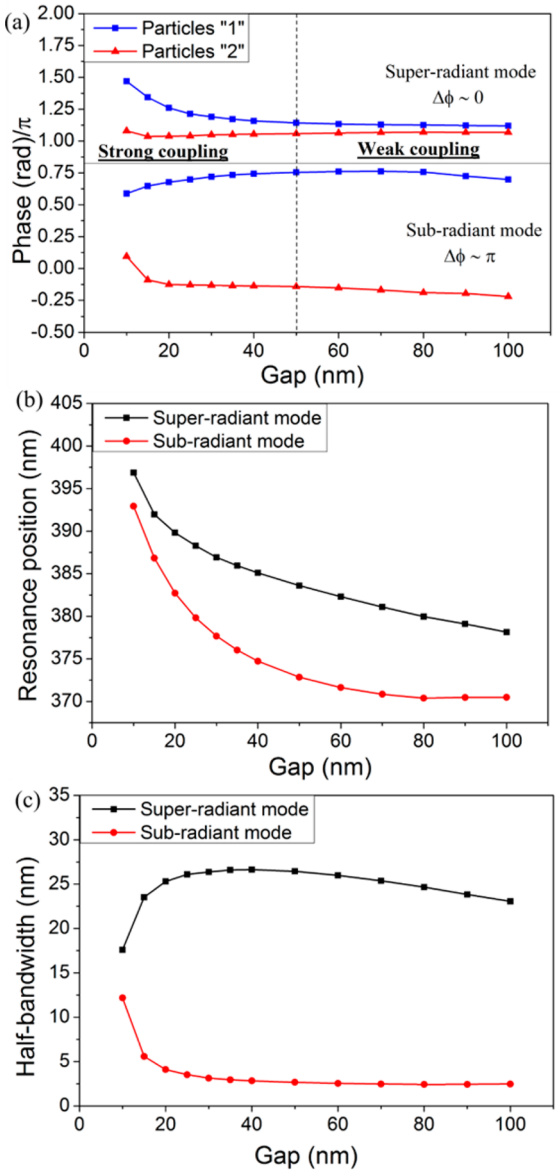


**Figure 7.** (a) Relative phase between dipolar moment oscillations, (b) resonance position, and (c) half-bandwidth of the hybrid mode in the quadrumer vs the gap of the dimer D2.

of the quadrumer extinction spectra in the weak coupling regime (Figure 8a) shows the redshift of the asymmetric Fano line profile when increasing the local refractive index. The plot of the two hybrid modes resonance positions in Figure 8b exhibits a nearly identical energy shift when increasing the surrounding medium refractive index, while the spectral width of the super-radiant mode increases much more significantly than the subradiant one (Figure 8c). The latter then retains its low radiative behavior. Using a linear regression of the energy shift versus the local refractive index and the subradiant mode fwhm in vacuum, the FoM of the Fano resonance in the weak coupling regime is estimated to 19.4, which is much larger than in previously studied finite structures.[18,27] By comparison, the FoM in the strong coupling regime is estimated to 6.7, demonstrating the advantage of a weak coupling configuration for sensing applications.

The Fano resonances in a quadrumer are observed when the particles are sufficiently large to ensure a sufficiently strong coupling between them. In the case of a quadrumer composed of smaller particles (studied in Supporting Information), the hybrid modes of the system also consist in a super-radiant and a subradiant modes, but without any marked asymmetric line profile.

## CONCLUSION

In this paper, we introduced the concept of complex valued extinction in a system of plasmonic particles. It provides a convenient way to characterize the resonant behavior of each particle of the system, and permits to determine the phase relations between the radiated fields. When considering the dipolar resonances of the particles, the partial complex valued extinctions can then be used to deduce the phase relations between the resultant dipolar moment oscillations.

We derived a set of coupled mode equations to describe the coupling behavior between two plasmon modes. A few phenomenological parameters have been introduced, among which the mutual coupling coefficients that allow a quantitative estimation of coupling strength in the coupled system. The proposed description, consistent with the coupled oscillator theory, predicts the hybridization of plasmon modes. The coupling between two modes forms two hybrid modes at different resonant positions depending on the coupling strengths. A fit of complex extinction spectra allows an accurate determination of all phenomenological parameters.

This approach was first applied to hybrid modes in dimers. The initial dipole modes of spheres couple to form hybrid modes differentiated by the direction of the dipole moment and the resulting phase relationship between the oscillations of the dipole moment of each particle. Thus, this system brings up bounding modes (where the dipolar moments are in an energetically favorable configuration, i.e., attractive), for which the spectral position is red-shifted when the interparticle coupling increases. Antibounding modes (with an energetically unfavorable, i.e., repulsive, configuration of dipolar moments) are also formed, with a spectral position shifted toward shorter wavelengths when the coupling increases. The modulus of mutual coupling coefficients shows a fast decreasing dependence with the gap between particles.

Finally, a more complex system consisting of four identical particles in interaction was investigated. The extinction of this system presents asymmetric profiles of Fano resonances. This kind of spectra is also well described using the coupled mode model. We characterized and identified the two hybrid modes resulting from the coupling between the initial dipolar modes of the particles. In the weak coupling regime of the system, corresponding to a large separation between two of the particles in the quadrumer, the Fano line profile emerges from the superposition of a broad super-radiant and a sharp subradiant modes. In the strong coupling regime, with a small distance between the particles, the subradiant mode as well as the resulting Fano resonance is broadened. The subradiant mode sharpness in the weak coupling regime results in a very high FoM, and this configuration appears to be the best suited for sensing applications.

In this work, we limited our analysis to the hybrid mode in systems composed of silver spheres. However, the developed approach can be extended to various particle geometries by using a numerical method (like the Discrete Dipole Approximation[28]) allowing the computation of the separated contribution of each particle in the system. The phenomenological model could also be extended to consider the coupling


DOI: 10.1021/ph500356n
ACS Photonics 2015, 2, 246−255

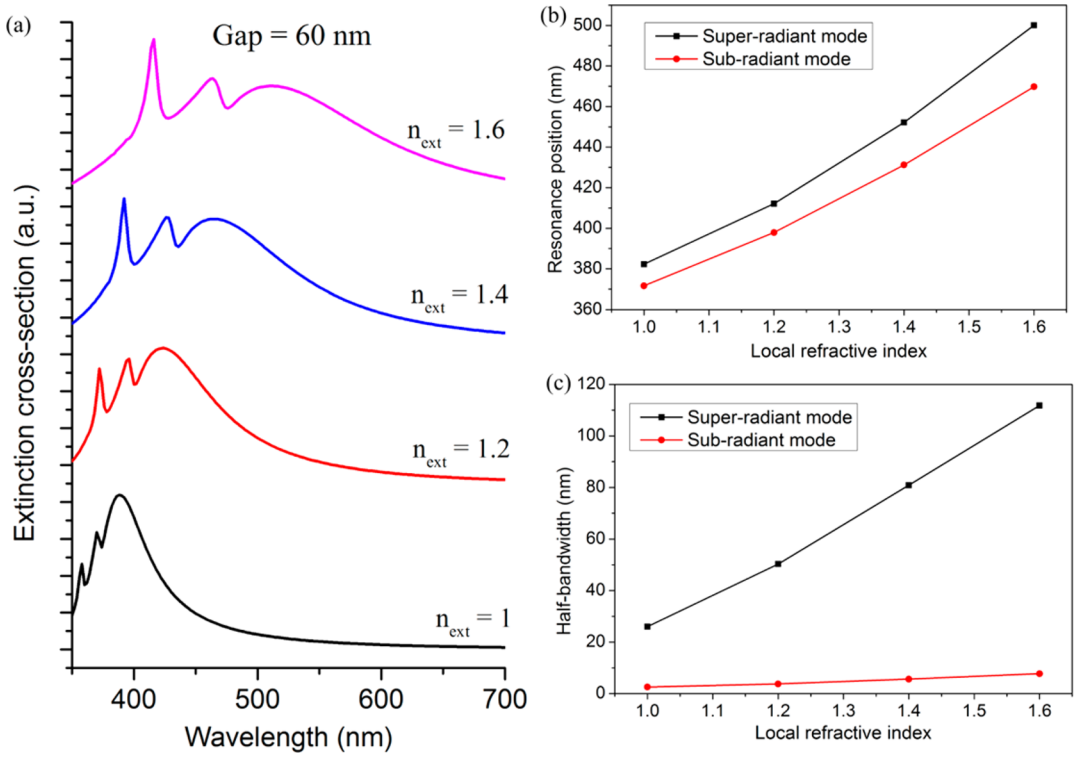


**Figure 8.** (a) Extinction spectrum of the quadrumer for different surrounding medium refractive indexes. (b) Resonance position and (c) half-bandwidth of the hybrid modes vs the local refractive index. A gap of 60 nm in the dimer D2 is fixed.

between dipolar and higher modes, or the coupling behavior in larger systems. In this case, the number of coupled equation (and then the number of phenomenological parameters) should be extended in consequence.

## METHODS

The rigorous calculation of the complex valued extinction relies on the resolution of the multiple scattering problem. The latter can be addressed as follows: let us consider an electromagnetic wave incident on a system of nonoverlapping particles with a given geometry, we search the wave scattered by this system which satisfies the Maxwell's equations by applying the boundary conditions on each interface. The superposition approach we use to solve this problem can be viewed as a generalization of the T-Matrix method,[29] and its expansion of electromagnetic fields in the basis of spherical functions, to multiple particle systems. Details relevant to the used method can be found in several papers dealing with the exact solution of multiple scattering in the case of spherical scatterers.[30−32]

For computations, we consider silver spheres with a refractive index obtained from the modified Drude model permittivity[1]

$$n_i^2 = \varepsilon_i(\omega) = \varepsilon_{ib} - \frac{\omega_p^2 \varepsilon_0}{\omega^2 + j\omega\Gamma} \tag{16}$$

with $\Gamma = \Gamma_0 + v_F/R_i$, the modified damping constant that takes account of the particle dimensions. $\Gamma_0$ is the damping constant of bulk silver ($\Gamma_0$ = 17.6 meV), $v_F$ is the Fermi velocity of electrons ($v_F = 1.39 \times 10^6$ m/s) and $R_i$ is the radius of the given sphere. $\varepsilon_{ib}$ is the contribution of interband transitions ($\varepsilon_{ib} = 3.7\varepsilon_0$, supposed to be constant in the visible spectrum), and $\omega_p$ is the plasma pulsation of silver ($\hbar\omega_p$ = 8.89 eV).

## ASSOCIATED CONTENT

### Supporting Information

Additional information, including the identification of dimer hybrid modes obtained when considering an incident polarization perpendicular to the dimer axis and the study of hybrid modes supported by a quadrumer composed of smaller silver spheres. This material is available free of charge via the Internet at http://pubs.acs.org.

## AUTHOR INFORMATION

### Corresponding Author

*E-mail: nathalie.destouches@univ-st-etienne.fr.

### Notes

The authors declare no competing financial interest.

## ACKNOWLEDGMENTS

This work was supported by the LABEX MANUTECH-SISE (ANR-10-LABX-0075) of Université de Lyon, within the program "Investissements d'Avenir" (ANR-11-IDEX-0007), operated by the French National Research Agency (ANR). The authors thank ANR for its financial support in the framework of Project PHOTOFLEX No. 12-NANO-0006, and the Rhône-Alpes region for the thesis grant of S.B.

## REFERENCES

(1) Kreibig, U.; Vollmer, M. *Optical Properties of Metal Clusters*; Springer: New York, 1995.
(2) Zhang, J.; Zhang, L. Nanostructures for Surface Plasmons. *Adv. Opt. Photonics* **2012**, *4*, 157−321.
(3) Mock, J. J.; Barbic, M.; Smith, D. R.; Schultz, D. A.; Schultz, S. Shape Effects in Plasmon Resonance of Individual Colloidal Silver Nanoparticles. *J. Chem. Phys.* **2002**, *116*, 6755−6759.



DOI: 10.1021/ph500356n
*ACS Photonics* 2015, 2, 246−255

(4) Noguez, C. Surface Plasmons on Metal Nanoparticles: The Influence of Shape and Physical Environment. *J. Phys. Chem. C* **2007**, *111*, 3806−3819.
(5) Mock, J. J.; Smith, D. R.; Schultz, S. Local Refractive Index Dependence of Plasmon Resonance Spectra from Individual Nanoparticles. *Nano Lett.* **2003**, *3*, 485−491.
(6) Lee, Y. H.; Chen, H.; Xu, Q.-H.; Wang, J. Refractive Index Sensitivities of Noble Metal Nanocrystals: The Effects of Multipolar Plasmon Resonances and the Metal Type. *J. Phys. Chem. C* **2011**, *115*, 7997−8004.
(7) Hao, E.; Schatz, G. C. Electromagnetic Fields around Silver Nanoparticles and Dimers. *J. Chem. Phys.* **2004**, *120*, 357−366.
(8) Anker, J. N.; Hall, W. P.; Lyandres, O.; Shah, N. C.; Zhao, J.; Van Duyne, R. P. Biosensing with Plasmonic Nanosensors. *Nat. Mater.* **2008**, *7*, 442−453.
(9) Kneipp, K.; Moskovits, M.; Kneipp, H. *Surface-Enhanced Raman Scattering: Physics and Applications*; Springer: New York, 2006.
(10) Maier, S. a.; Brongersma, M. l.; Kik, P. g.; Meltzer, S.; Requicha, A. a. g.; Koel, B. e.; Atwater, H. a. Plasmonics: A Route to Nanoscale Optical Devices (Advanced Materials, 2001, 13, 1501). *Adv. Mater.* **2003**, *15*, 562−562.
(11) Clavero, C. Plasmon-Induced Hot-Electron Generation at Nanoparticle/Metal-Oxide Interfaces for Photovoltaic and Photocatalytic Devices. *Nat. Photonics* **2014**, *8*, 95−103.
(12) Prodan, E.; Radloff, C.; Halas, N. J.; Nordlander, P. A Hybridization Model for the Plasmon Response of Complex Nanostructures. *Science* **2003**, *302*, 419−422.
(13) Nordlander, P.; Oubre, C.; Prodan, E.; Li, K.; Stockman, M. I. Plasmon Hybridization in Nanoparticle Dimers. *Nano Lett.* **2004**, *4*, 899−903.
(14) Wang, H.; Brandl, D. W.; Nordlander, P.; Halas, N. J. Plasmonic Nanostructures: Artificial Molecules. *Acc. Chem. Res.* **2007**, *40*, 53−62.
(15) Luk'yanchuk, B.; Zheludev, N. I.; Maier, S. A.; Halas, N. J.; Nordlander, P.; Giessen, H.; Chong, C. T. The Fano Resonance in Plasmonic Nanostructures and Metamaterials. *Nat. Mater.* **2010**, *9*, 707−715.
(16) Rahmani, M.; Luk'yanchuk, B.; Hong, M. Fano Resonance in Novel Plasmonic Nanostructures. *Laser Photon. Rev.* **2013**, *7*, 329−349.
(17) Miroshnichenko, A. E.; Flach, S.; Kivshar, Y. S. Fano Resonances in Nanoscale Structures. *Rev. Mod. Phys.* **2010**, *82*, 2257−2298.
(18) Mirin, N. A.; Bao, K.; Nordlander, P. Fano Resonances in Plasmonic Nanoparticle Aggregates. *J. Phys. Chem. A* **2009**, *113*, 4028−4034.
(19) Hao, F.; Sonnefraud, Y.; Dorpe, P. V.; Maier, S. A.; Halas, N. J.; Nordlander, P. Symmetry Breaking in Plasmonic Nanocavities: Subradiant LSPR Sensing and a Tunable Fano Resonance. *Nano Lett.* **2008**, *8*, 3983−3988.
(20) Verellen, N.; Sonnefraud, Y.; Sobhani, H.; Hao, F.; Moshchalkov, V. V.; Dorpe, P. V.; Nordlander, P.; Maier, S. A. Fano Resonances in Individual Coherent Plasmonic Nanocavities. *Nano Lett.* **2009**, *9*, 1663−1667.
(21) Mackowski, D. W. Calculation of Total Cross Sections of Multiple-Sphere Clusters. *J. Opt. Soc. Am.* **1994**, *11*, 2851−2861.
(22) Haus, H. A. *Waves and Fields in Optoelectronics*; Prentice Hall: Upper Saddle River, NJ, 1984.
(23) Bakhti, S.; Destouches, N.; Tishchenko, A. V. Analysis of Plasmon Resonances on a Metal Particle. *J. Quant. Spectrosc. Radiat. Transfer* **2014**, *146*, 113−122.
(24) Tishchenko, A. V.; Parriaux, O. M.; Neuschafer, D. Waveguide Grating Coupling of 2D Focused Beam Under Normal Incidence: a Phenomenological Approach. *Proc. SPIE* **2004**, *5249*, 546−556.
(25) Novotny, L. Strong Coupling, Energy Splitting, and Level Crossings: A Classical Perspective. *Am. J. Phys.* **2010**, *78*, 1199−1202.
(26) Sherry, L. J.; Chang, S.-H.; Schatz, G. C.; Van Duyne, R. P.; Wiley, B. J.; Xia, Y. Localized Surface Plasmon Resonance Spectroscopy of Single Silver Nanocubes. *Nano Lett.* **2005**, *5*, 2034−2038.
(27) Lassiter, J. B.; Sobhani, H.; Fan, J. A.; Kundu, J.; Capasso, F.; Nordlander, P.; Halas, N. J. Fano Resonances in Plasmonic Nanoclusters: Geometrical and Chemical Tunability. *Nano Lett.* **2010**, *10*, 3184−3189.
(28) Draine, B. T.; Flatau, P. J. Discrete-Dipole Approximation for Scattering Calculations. *J. Opt. Soc. Am.* **1994**, *11*, 1491−1499.
(29) Doicu, A.; Wriedt, T.; Eremin, Y. A. *Light Scattering by Systems of Particles; Null-Field Method with Discrete Sources: Theory And*; Springer: New York, 2006.
(30) Mackowski, D. W. Analysis of Radiative Scattering for Multiple Sphere Configurations. *Proc. R. Soc. London, Ser. A* **1991**, *433*, 599−614.
(31) Mackowski, D. The Extension of Mie Theory to Multiple Spheres. In *The Mie Theory*; Springer Series in Optical Sciences; Hergert, W., Wriedt, T., Eds.; Springer: Berlin; Heidelberg, 2012; pp 223−256.
(32) Xu, Y. Electromagnetic Scattering by an Aggregate of Spheres. *Appl. Opt.* **1995**, *34*, 4573.


DOI: 10.1021/ph500356n
*ACS Photonics* 2015, 2, 246−255